

Probing negative values of a Wigner function in scattering of Schrödinger cats by atoms

Dmitry V. Karlovets¹ and Valeriy G. Serbo^{2,3}

¹ Tomsk State University, Lenina 36, 634050 Tomsk, Russia

² Novosibirsk State University, Pirogova 2, RUS-630090, Novosibirsk, Russia

³ Sobolev Institute of Mathematics, Koptyuga 4, RUS-630090, Novosibirsk, Russia

Abstract

Within a plane-wave approximation in scattering, an incoming wave packet's Wigner function stays everywhere positive, which obscures such quantum phenomena as non-locality and entanglement. With the advent of the modern electron microscopes with subnanometer-sized beams one can enter the genuinely quantum regime where the latter effects become only moderately attenuated. Here we show how to probe negative values of the Wigner function in scattering of a coherent superposition of two Gaussian packets with a non-vanishing impact-parameter between them (a Schrödinger's cat state) by atomic targets. For hydrogen in the ground $1s$ state, a small parameter of the problem, a ratio a/σ_{\perp} of the Bohr radius a to the beam width σ_{\perp} , is no longer vanishing. We predict an azimuthal asymmetry of the scattered electrons, which is found to be up to 10% when the impact-parameter is comparable to the beam width, and argue that it can be reliably detected. Production of subnanometer-sized Schrödinger's cat states and probing such purely quantum effects can open new perspectives in studying the interiors of atoms.

1 Introduction

There are not many examples where the widely used plane-wave approximation in scattering fails to work, see [1–7]. The incoming wave packets' density matrices in phase space, the Wigner functions [8], turn out to be everywhere positive in the plane-wave regime, whereas their negative values may become prominent only when the beams are focused to a spot comparable to the Compton wave length, $\sigma_{\perp} \sim \lambda_c = \hbar/(mc)$, where m is the particle's mass [6]. However, when the wave function is not Gaussian or it represents a coherent superposition of packets, the genuine quantum effects arising from the Wigner function's possible negativity, such as non-locality and entanglement, may become noticeable at much larger scales. A simplest example here is a superposition of two coherent states separated by an impact parameter $2\mathbf{r}_0$, $|\mathbf{r}_0\rangle \pm |-\mathbf{r}_0\rangle$, the so-called Schrödinger's cat state widely used in quantum optics where the negative values of its Wigner function are successfully measured [9–11] and even teleported [12]. Other examples of the systems with the not-everywhere positive Wigner functions embrace ensembles of thousands of cold entangled atoms [13], ultracold quantum bosonic gases [14], twisted photons [15], etc.

Here we show that scattering of a similar electronic cat state by atoms reveals quantum interference effects, inaccessible in the plane-wave approximation or even in the paraxial regime with the everywhere positive Wigner functions. Applying a theory recently developed by us in [16, 17], we demonstrate that a small parameter of the problem turns out to be a ratio of the potential radius a to the beam width σ_\perp , which is $1/\alpha \approx 137$ times higher than λ_c/σ_\perp for hydrogen ($a \approx 0.053$ nm is a Bohr radius). As beams of the modern electron microscopes have already been focused to an Ångström size spot [18], one can enter a genuinely quantum regime of scattering where the projectiles behave like true quantum systems with the probability density being spatially inhomogeneous on the atomic scale. One may call this a *deeply non-plane-wave* regime, in which the Wigner functions are treated *non-perturbatively* (cf. [6]) and the packets' width in the momentum space is not necessarily vanishingly small. In contrast to the conventional scattering, effects of the possible non-locality and entanglement are only moderately attenuated here.

As a hallmark of strong non-classicality, we predict an azimuthal asymmetry of the scattered electrons. For non-relativistic but fast electrons focused to a subnanometer spot, the asymmetry reaches the values of 10%, which can be reliably detected with existing technology. The effect vanishes for very wide beams, $a/\sigma_\perp \rightarrow 0$, and when the impact parameter between the two Gaussians of the cat state is too large, $r_0 \gg \sigma_\perp$. Quantum beams of massive particles (first of all, of electrons) with the not-everywhere positive Wigner functions can become a useful tool for probing the interiors of atoms and molecules, as well as for quantum information purposes, along with the vortex electrons for instance, and for solid-state physics. For the sake of brevity, we set $\hbar = 1$. All vectors, except \mathbf{Q} and \mathbf{p}_f , have two components: $\mathbf{p} \equiv \{p_x, p_y, 0\}$.

2 Wigner function of a Schrödinger's cat state

Consider a system of two Gaussian wave packets moving along the z axis with the same mean momentum $\{0, 0, p_i\}$, with the coordinate uncertainties σ_z and σ_\perp , and separated by a distance $2\mathbf{r}_0 \equiv 2\{x_0, y_0, 0\}$. Its transverse wave function in the momentum representation is a coherent superposition of two one-particle packets:

$$\psi_{1\pm 1}(\mathbf{p}; \mathbf{r}_0) = \frac{1}{\sqrt{2}} \frac{\psi_1(\mathbf{p})}{\sqrt{1 \pm \exp\{-\mathbf{r}_0^2/(2\sigma_\perp^2)\}}} (e^{-i\mathbf{r}_0\mathbf{p}} \pm e^{i\mathbf{r}_0\mathbf{p}}), \quad \int d^2p |\psi_{1\pm 1}(\mathbf{p})|^2 = 1, \quad (1)$$

where

$$\psi_1(\mathbf{p}) = \sqrt{\frac{2\sigma_\perp^2}{\pi}} \exp\{-\sigma_\perp^2 \mathbf{p}^2\}, \quad \int d^2p |\psi_1(\mathbf{p})|^2 = 1, \quad (2)$$

is a wave function of one packet. We will call the states ψ_{1+1} and ψ_{1-1} *an even cat state* and *an odd one*, respectively. The corresponding Wigner function at $t = 0$ is (see, for instance, [19])

$$\begin{aligned} W_{1\pm 1}(\mathbf{r}, \mathbf{p}) &= \int \frac{d^2k}{(2\pi)^2} e^{i\mathbf{k}\mathbf{r}} \psi_{1\pm 1}^*(\mathbf{p} - \mathbf{k}/2) \psi_{1\pm 1}(\mathbf{p} + \mathbf{k}/2) = \\ &= \frac{W_1(\mathbf{r}, \mathbf{p})}{1 \pm \exp\{-\mathbf{r}_0^2/(2\sigma_\perp^2)\}} \left(\cosh(\mathbf{r}_0\mathbf{r}/\sigma_\perp^2) e^{-\mathbf{r}_0^2/(2\sigma_\perp^2)} \pm \cos(2\mathbf{r}_0\mathbf{p}) \right), \end{aligned} \quad (3)$$

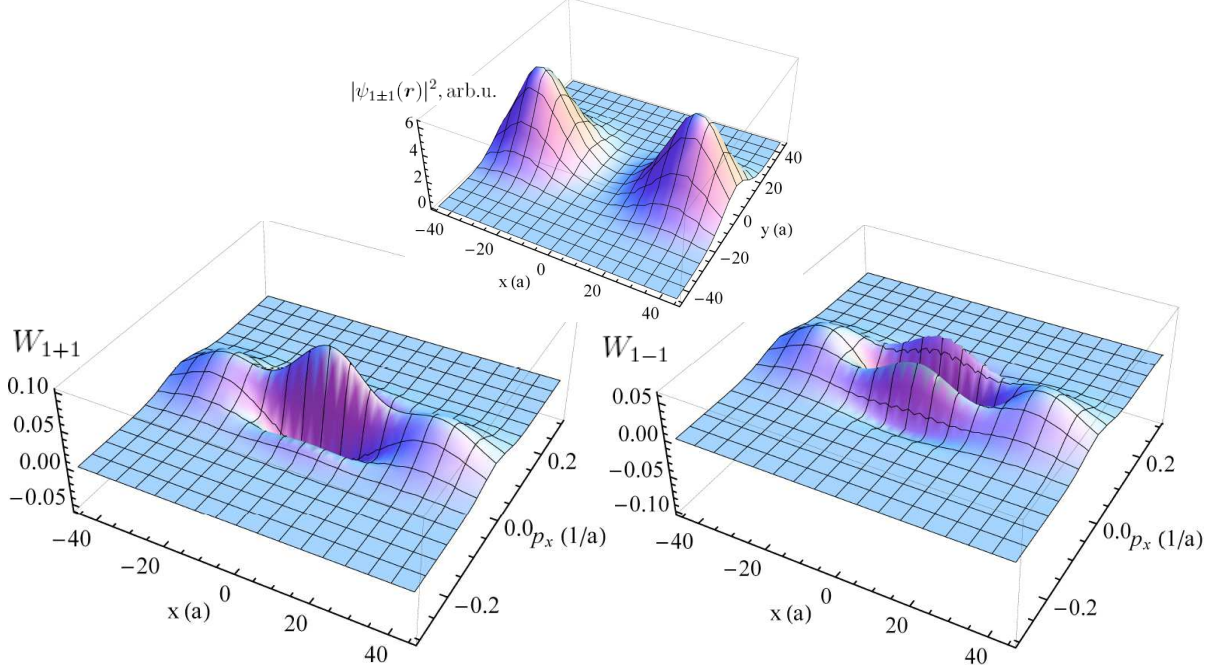


Figure 1: Wigner functions of the electronic Schrödinger cat state (3) with $x_0 = 3\sigma_\perp$ and $\sigma_\perp = 10a$. Left: an even cat state, right: an odd cat state. The upper panel shows the probability density, $|\psi_{1\pm 1}(\mathbf{r})|^2 = \int d^2p W_{1\pm 1}$. Parameters: $y = y_0 = p_y = 0$, $p_z = p_i = 10/a$ ($\varepsilon_{\text{kin}} = 1.4$ keV).

where

$$W_1(\mathbf{r}, \mathbf{p}) = \frac{1}{\pi^2} \exp \left\{ -2\sigma_\perp^2 \mathbf{p}^2 - \mathbf{r}^2 / (2\sigma_\perp^2) \right\} \quad (4)$$

is an everywhere-positive Wigner function of one packet.

It is the last term in the parentheses, $\cos(2\mathbf{r}_0\mathbf{p})$, that is responsible for possible negativity in some regions of the phase space. The function W_{1+1} turns negative when

$$r_0 \gtrsim \sigma_\perp \sim 1/p_\perp,$$

i.e. the distance between the two packets gets larger than the packet's width σ_\perp (see Fig.1), but stays everywhere positive when $r_0 \lesssim \sigma_\perp$ (see Fig.2). The function W_{1-1} , on the contrary, has prominent negative regions even when $r_0 \approx \sigma_\perp$. For smaller values, $r_0 < \sigma_\perp$, the odd cat state, unlike the even one, reveals a somewhat fermionic behavior with the Gaussians staying separated by the distance $\approx 2\sigma_\perp$, as shown in Fig.2. That is why we will stick to the case $r_0 \geq \sigma_\perp$ for the odd cat in what follows.

In an *incoherent* mixture of two one-particle Wigner functions,

$$\frac{1}{2} (W_1(\mathbf{r}, \mathbf{p}; \mathbf{r}_0) + W_1(\mathbf{r}, \mathbf{p}; -\mathbf{r}_0)) \propto \cosh(\mathbf{r}_0\mathbf{r}/\sigma_\perp^2), \quad (5)$$

which takes place for mixed states for instance [19], the interference term is absent. As a result, this sum stays everywhere positive and looks exactly like the probability density shown in the upper panel of Fig.1.

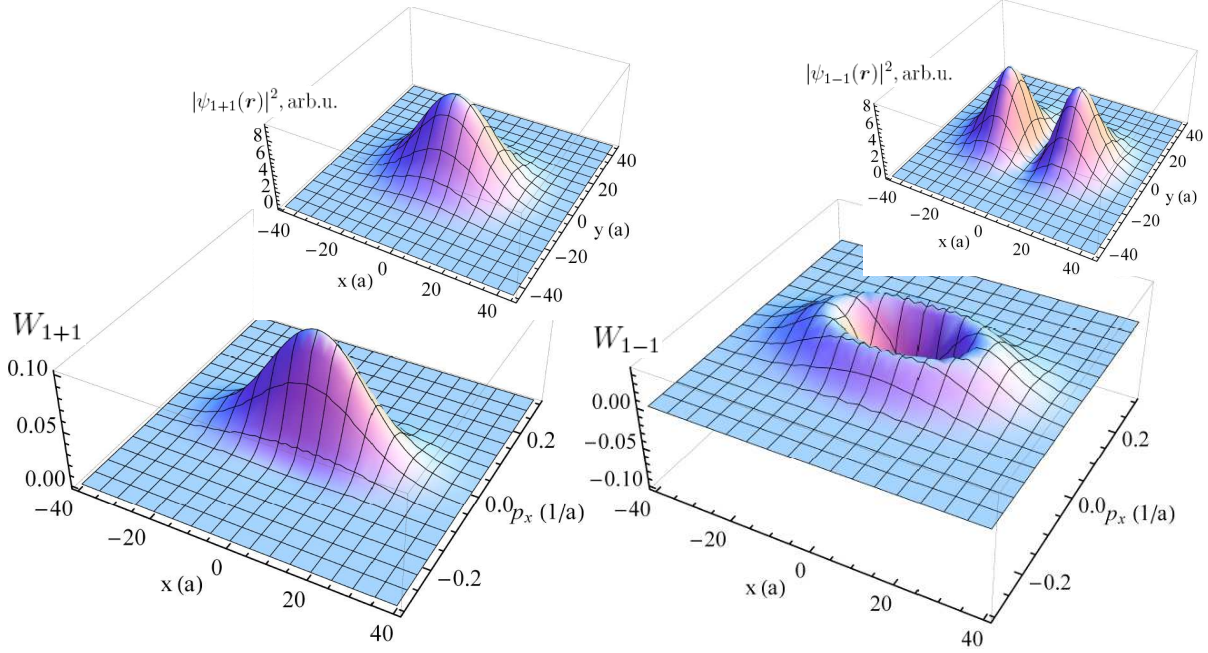


Figure 2: The same as in Fig.1 but for $x_0 = \sigma_{\perp}$.

3 Scattering of a Schrödinger's cat by atoms

Let us now study elastic scattering of such a system off a central potential with a radius a in the Born approximation. We consider an experimentally relevant scenario in which (i) the packet's longitudinal size σ_z is larger than the field radius, $\sigma_z \gg a$, and (ii) the packet's dispersion in the transverse plane is negligible during the collision, that is, $t_{\text{dis}} \sim \sigma_{\perp}/v_{\perp} \gg t_{\text{col}} \sim \sigma_z/v_z$. Under these assumptions, which can be rewritten as

$$a \ll \sigma_z \ll \sigma_{\perp}^2 p_i, \quad (6)$$

the scattering amplitude is given by Eqs.(29),(30) of the Ref. [16] where one can put $\theta_k = 0$, as $\theta_k \approx 1/(\sigma_{\perp} p_i) \ll 1$.

Then instead of a single scatterer we take a realistic target with a density of atoms $n(\mathbf{b})$, normalized as $\int d^2b n(\mathbf{b}) = 1$, and with a width $\sigma_t \gg a$. A number of scattering events for an incident beam of N_e electrons, according to Eq.(41) from Ref. [17], can be represented as follows:

$$\frac{d\nu}{d\Omega} = N_e \int d^2b n(\mathbf{b}) \frac{d^2p}{2\pi} \frac{d^2k}{2\pi} e^{i\mathbf{b}\mathbf{k}} f(\mathbf{Q} - \mathbf{p} - \mathbf{k}/2) f^*(\mathbf{Q} - \mathbf{p} + \mathbf{k}/2) \times \psi(\mathbf{p} + \mathbf{k}/2) \psi^*(\mathbf{p} - \mathbf{k}/2), \quad (7)$$

where we have changed the variables: $\mathbf{k}_{\perp}, \mathbf{k}'_{\perp} \rightarrow \mathbf{p} = (\mathbf{k}_{\perp} + \mathbf{k}'_{\perp})/2, \mathbf{k} = \mathbf{k}_{\perp} - \mathbf{k}'_{\perp}$, and $\mathbf{Q} = \mathbf{p}_f - p_i \hat{z}$ with \mathbf{p}_f being a 3D momentum of the final (plane-wave) electron:

$$\mathbf{Q}_z = p_f \cos \theta - p_i, \quad \mathbf{Q}_{\perp} = p_f \sin \theta \{\cos \varphi, \sin \varphi, 0\}.$$

Finally, a real function $f(\mathbf{Q})$ is the scattering amplitude in the Born approximation.

When the density $n(\mathbf{b})$ varies at distances of the order of $\sigma_t \gg a$, only the small values of $k \lesssim 1/\sigma_t \ll 1/a$ contribute to the integral. Therefore one can expand the amplitudes

as follows:

$$f(\mathbf{Q} - \mathbf{p} - \mathbf{k}/2)f^*(\mathbf{Q} - \mathbf{p} + \mathbf{k}/2) = |f(\mathbf{Q} - \mathbf{p})|^2 + \mathcal{O}(k^2 a^2), \quad k^2 a^2 \lesssim a^2/\sigma_t^2.$$

Within this accuracy, the integral over \mathbf{k} brings the projectile's Wigner function $W(\mathbf{b}, \mathbf{p})$ and we arrive at the following simple formula:

$$\frac{d\nu}{d\Omega} = N_e \int d^2b d^2p n(\mathbf{b}) W(\mathbf{b}, \mathbf{p}) |f(\mathbf{Q} - \mathbf{p})|^2. \quad (8)$$

Clearly, possible negative values of the Wigner function *diminish* the number of events.

When the target is homogeneous and very wide, one can put

$$n(\mathbf{b}) = \frac{\theta(R - b)}{\pi R^2}$$

and the corresponding number of events,

$$\frac{d\nu}{d\Omega} = \frac{N_e}{\pi R^2} \int d^2p |\psi(\mathbf{p})|^2 |f(\mathbf{Q} - \mathbf{p})|^2, \quad |\psi(\mathbf{p})|^2 = \int d^2b W(\mathbf{b}, \mathbf{p}), \quad (9)$$

reproduces Eq.(38) from Ref. [16].

As a simplest example we take a packet with the everywhere positive Wigner function (4) scattered by a Gaussian target with

$$n(\mathbf{b}) = \frac{1}{2\pi\sigma_t^2} e^{-(\mathbf{b}-\mathbf{b}_0)^2/(2\sigma_t^2)}.$$

The result is

$$\frac{d\nu_1}{d\Omega} = \frac{N_e\sigma_\perp^2}{\pi^2\Sigma^2} e^{-b_0^2/(2\Sigma^2)} \int d^2p |f(\mathbf{Q} - \mathbf{p})|^2 e^{-2\sigma_\perp^2 p^2}, \quad (10)$$

where

$$\Sigma^2 = \sigma_t^2 + \sigma_\perp^2.$$

As can be readily seen, this expression *does not* depend on the azimuthal scattering angle φ , as one can substitute $\varphi_p - \varphi \rightarrow \varphi_p$, even if the target's center \mathbf{b}_0 does not coincide with the one of the incident packet. Such *an azimuthal degeneracy* is a consequence of the Born approximation and the condition of the wide target. Likewise, there is no azimuthal dependence for an incoherent sum of the packets (5).

In order to restore this dependence one should either go beyond the first Born approximation or take a coherent sum of the incident packets with a Wigner function that is not necessarily everywhere positive. In the latter case, we take the Schrödinger cat (3) and the same Gaussian target. This time we obtain

$$\begin{aligned} \frac{d\nu_{1\pm 1}}{d\Omega} &= N_e \frac{\sigma_\perp^2}{\pi^2\Sigma^2} \frac{\exp\{-\mathbf{b}_0^2/(2\Sigma^2)\}}{1 \pm \exp\{-r_0^2/(2\sigma_\perp^2)\}} \int d^2p |f(\mathbf{Q} - \mathbf{p})|^2 e^{-2\sigma_\perp^2 p^2} \\ &\times \left(\cosh(\mathbf{b}_0 \mathbf{r}_0/\Sigma^2) \exp\{-r_0^2/(2\Sigma^2)\} \pm \cos(2\mathbf{r}_0 \mathbf{p}) \right). \end{aligned} \quad (11)$$

As a specific example, we take a target made of hydrogen in the ground 1s state for which

$$f(\mathbf{p}) = \frac{a}{2} \left(\frac{1}{1 + (a/2)^2 \mathbf{p}^2} + \frac{1}{(1 + (a/2)^2 \mathbf{p}^2)^2} \right).$$

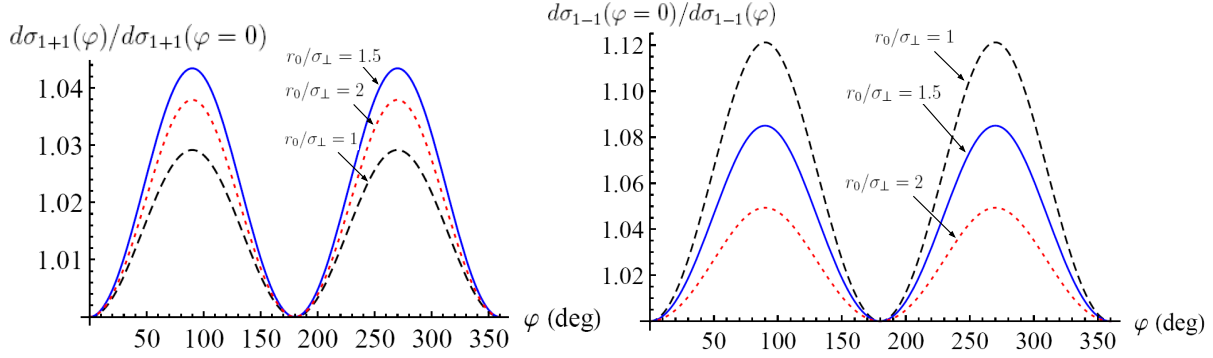


Figure 3: Azimuthal asymmetry of the electrons scattered by a wide hydrogenic target for $\sigma_{\perp} = 2a \approx 0.1$ nm (FWHM ≈ 0.25 nm), $\theta = 10^\circ$, $r_0/\sigma_{\perp} = 1$ (black dashed line), 1.5 (blue solid line), 2 (red dotted line). Parameters: $\sigma_t \gg \sigma_{\perp}$, $\varphi_{r_0} = 0$, $p_i = p_f = 10/a$ ($\varepsilon_{\text{kin}} = 1.4$ keV).

Then using Eq.(54) from Ref. [16] we can integrate over \mathbf{p} and get the following final result:

$$\begin{aligned} \frac{d\nu_{1\pm 1}}{d\Omega} = \mathcal{N}_{1\pm 1} \int_0^{\infty} dx e^{-xg} \frac{x + x^2 + x^3/6}{1 + xa^2/(8\sigma_{\perp}^2)} & \left(\cosh\left(\frac{\mathbf{b}_0 \mathbf{r}_0}{\Sigma^2}\right) e^{-r_0^2/(2\Sigma^2)} \pm \right. \\ & \left. \pm \cos\left(2\mathbf{r}_0 \mathbf{p}_f \frac{xa^2/(8\sigma_{\perp}^2)}{1 + xa^2/(8\sigma_{\perp}^2)}\right) \exp\left\{-\frac{r_0^2}{2\sigma_{\perp}^2(1 + xa^2/(8\sigma_{\perp}^2))}\right\} \right), \end{aligned} \quad (12)$$

where

$$\mathcal{N}_{1\pm 1} = \frac{N_e}{2\pi\Sigma^2} \left(\frac{a}{2}\right)^2 \frac{e^{-b_0^2/(2\Sigma^2)}}{1 \pm e^{-r_0^2/(2\sigma_{\perp}^2)}}, \quad g = 1 + \left(\frac{a}{2}\right)^2 \left(Q_z^2 + \frac{Q_{\perp}^2}{1 + xa^2/(8\sigma_{\perp}^2)}\right). \quad (13)$$

One may call

$$\frac{d\sigma_{1\pm 1}}{d\Omega} = \frac{2\pi\Sigma^2}{N_e} \frac{d\nu_{1\pm 1}}{d\Omega}$$

an effective cross section, as it stays finite for the very wide target, $\Sigma \approx \sigma_t \rightarrow \infty$.

The interference term in (12) turns to unity for the wide packets and a small target, $a \ll \sigma_{\perp}$, but for the wide target and the well-focused packets, $\sigma_t \gg \sigma_{\perp} \gtrsim a$, it results in *an azimuthal asymmetry*. This asymmetry of the scattered electrons exists only for the moderate distances between the packets,

$$r_0 \gtrsim \sigma_{\perp} \gtrsim a,$$

and it vanishes when either $r_0 \rightarrow 0$ (for an even cat state, for an odd one this limit has no sense) or $r_0 \gg \sigma_{\perp}$. Two wave packets of electrons focused to $\sigma_{\perp} \sim 0.1$ nm, as in the experiment [18], and separated by a comparable distance can do the job.

As shown in Figs. 3, 4, an azimuthal variation of the cross section can reach 10% for such beams. Clearly, the effect is stronger for the odd cat state with $r_0 \approx \sigma_{\perp}$, but for $r_0 = 2\sigma_{\perp} - 3\sigma_{\perp}$ it is nearly the same as for the even cat. Width of the distributions over the scattering angle θ in Fig.4 is determined by the packet's mean momentum. For higher energies, the peak shifts to smaller angles (it's around 5° for $p_i = 30/a$), whereas for lower

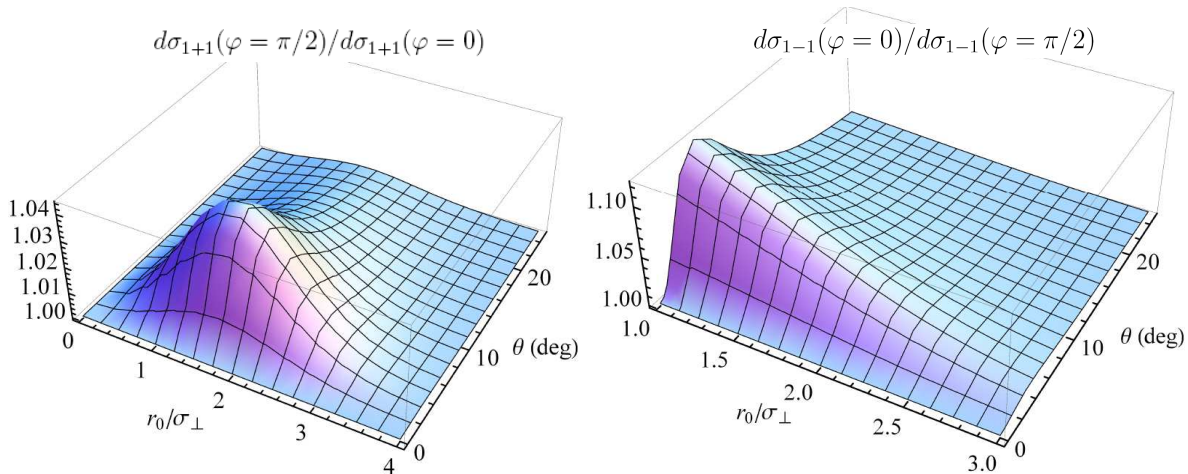


Figure 4: Azimuthal asymmetry for the same parameters as in Fig.3 but with $p_i = p_f = 20/a$.

ones it moves to larger polar angles and widens. Meanwhile, the value of the azimuthal asymmetry persists.

With the increasing beam width σ_{\perp} , the asymmetry drops as σ_{\perp}^{-2} . For instance, for $\sigma_{\perp} = 4a$ (FWHM ≈ 0.5 nm) it is 0.1% – 1%. With high statistics, which is feasible in atomic collisions with subnanometer-sized wave packets [7], such variations can be reliably detected.

4 Summary

Unlike cats, Gaussian beams are azimuthally symmetric entities with the everywhere positive Wigner functions. The coherent superposition of two of them no longer possesses this property and the negative values of its Wigner function become prominent when the quantum interference gets strong. In this regime, scattering of such a cat state by atoms reveals the azimuthal asymmetry, a phenomenon accessible neither in the paraxial (plane wave) approximation nor in the quasi-classical regime. As beams of the modern electronic microscopes can already be focused to a subnanometer-sized spot, detection of this purely quantum effect is feasible with existing technology. For hydrogenic targets, we predict the asymmetry of the order of 1% – 10% when the impact-parameter between the two Gaussians of the cat state does not exceed the beam width much.

Although fulfillment of the latter requirement seems challenging (but not unfeasible), production of such quantum beams of massive particles with the Wigner functions that are not everywhere positive can provide access to the previously unexplored ultra-quantum regime of scattering, thus giving us new tools for atomic physics, quantum information, and solid-state physics. Along with the Schrödinger’s cat, these beams may include coherent superpositions of the vortex electrons, of Airy beams [20], etc.

We are grateful to V. G. Bagrov and A. K. Gutakovskii for useful discussions. D.K. is supported by the Competitiveness Improvement Program of the Tomsk State University. V.G.S. is supported by the Russian Foundation for Basic Research via Grant No. 15-02-06444. D.K. also wishes to thank the Alexander von Humboldt Foundation (Germany).

References

- [1] I. G. Halliday, R. R. Beever, C. J. Maxwell, Wave packets and the space-time structure of production processes, Nucl. Phys. B **149**, 61 (1979).
- [2] G.L. Kotkin, V.G. Serbo, A. Schiller, Processes with large impact parameters at colliding beams, Int. J. Mod. Phys. A **7**, 4707 (1992).
- [3] K. Melnikov, V.G. Serbo, Processes with a t -channel singularity in the physical region: finite beam sizes make cross sections finite, Nucl. Phys. B **483**, 67 (1997).
- [4] E.Kh. Akhmedov, A. Yu. Smirnov, Paradoxes of neutrino oscillations, Phys. Atom. Nucl. **72**, 1363 (2009); arXiv:0905.1903 [hep-ph].
- [5] E.Kh. Akhmedov, J. Kopp, Neutrino oscillations: Quantum mechanics vs. quantum field theory, J. High Energy Phys. **04**, 008 (2010).
- [6] D.V. Karlovets, Scattering of wave packets with phases, J. High Energy Phys. **03**, 049 (2017).
- [7] M. Schulz, The Role of Projectile Coherence in the Few-Body Dynamics of Simple Atomic Systems, Advances in Atomic, Molecular, and Optical Physics (2017), in press, <http://dx.doi.org/10.1016/bs.aamop.2017.01.001>.
- [8] E. Wigner, On the quantum correction for thermodynamic equilibrium, Phys. Rev. **40**, 749 (1932).
- [9] A. Ourjoumtsev, H. Jeong, R. Tualle-Brouri, et al., Generation of optical "Schrödinger cats" from photon number states, Nature **448**, 784 (2007).
- [10] K. Laiho, K.N. Cassemiro, D. Gross, et al., Probing the Negative Wigner Function of a Pulsed Single Photon Point by Point, Phys. Rev. Lett. **105**, 253603 (2010).
- [11] T. Douce, A. Eckstein, S.P. Walborn, et al., Direct measurement of the biphoton Wigner function through two-photon interference, Scientific Reports **3**, 3530 (2013).
- [12] N. Lee, H. Benichi, Y. Takeno, et al., Teleportation of Nonclassical Wave Packets of Light, Science **332**, 330 (2011).
- [13] R. McConnell, H. Zhang, J. Hu, et al., Entanglement with negative Wigner function of almost 3000 atoms heralded by one photon, Nature **519**, 439 (2015).
- [14] U.R. Fischer, M.-K. Kang, "Photonic" Cat States from Strongly Interacting Matter Waves, Phys. Rev. Lett. **115**, 260404 (2015).
- [15] M. Mirhosseini, O. S. Magaña-Loaiza, C. Chen, et al., Wigner Distribution of Twisted Photons, Phys. Rev. Lett. **116**, 130402 (2016).
- [16] D.V. Karlovets, G.L. Kotkin, and V.G. Serbo, Scattering of wave packets on atoms in the Born approximation, Phys. Rev. A **92**, 052703 (2015).

- [17] D. V. Karlovets, G. L. Kotkin, V. G. Serbo, A. Surzhykov, Scattering of twisted electron wave packets by atoms in the Born approximation, *Phys. Rev. A* **95**, 032703 (2017).
- [18] J. Verbeeck, P. Schattschneider, S. Lazar, et al., Atomic scale electron vortices for nanoresearch, *Appl. Phys. Lett.* **99**, 203109 (2011).
- [19] W. B. Case, Wigner functions and Weyl transforms for pedestrians, *Am. J. Phys.* **76**, 937 (2008).
- [20] N. Voloch-Bloch, Y. Lereah, Y. Lilach, et al., Generation of electron Airy beams, *Nature* **494**, 331 (2013).